



CHORUS

This is the accepted manuscript made available via CHORUS. The article has been published as:

Out-of-time-order correlation in marginal many-body localized systems

Kevin Slagle, Zhen Bi, Yi-Zhuang You, and Cenke Xu

Phys. Rev. B **95**, 165136 — Published 24 April 2017

DOI: [10.1103/PhysRevB.95.165136](https://doi.org/10.1103/PhysRevB.95.165136)

Out-of-Time-Order Correlation in Marginal Many-Body Localized Systems

Kevin Slagle,¹ Zhen Bi,¹ Yi-Zhuang You,^{1,2} and Cenke Xu¹

¹*Department of Physics, University of California,
Santa Barbara, CA 93106, USA*

²*Department of Physics, Harvard University,
Cambridge, MA 02138, USA*

We show that the out-of-time-order correlation (OTOC) $\langle W(t)^\dagger V(0)^\dagger W(t)V(0) \rangle$ in many-body localized (MBL) and marginal MBL systems can be efficiently calculated by the spectrum bifurcation renormalization group (SBRG). We find that in marginal MBL systems, the scrambling time t_{scr} follows a stretched exponential scaling with the distance d_{WV} between the operators W and V : $t_{\text{scr}} \sim \exp(\sqrt{d_{WV}/l_0})$, which demonstrates Sinai diffusion of quantum information and the enhanced scrambling by the quantum criticality in non-chaotic systems.

The out-of-time-order correlation (OTOC)¹⁻⁷ was recently proposed to quantify the scrambling and the butterfly effect in quantum many-body dynamics, and has attracted great research interests in quantum gravity⁸⁻¹¹, quantum information¹² and condensed matter¹³⁻¹⁷ communities. Consider two local unitary operators W and V , along with the many-body Hamiltonian H of the system; the OTOC is defined as

$$F(t) = \langle W(t)^\dagger V(0)^\dagger W(t)V(0) \rangle, \quad (1)$$

where $W(t) = e^{iHt}W e^{-iHt}$ and $V(0) = V$ are the operators at time t and time 0 respectively. The notation $\langle \dots \rangle$ stands for either the expectation value on a pure state of interest (typically a short-range entangled state), or the ensemble average over a mixed state density matrix. The OTOC is closely related to the squared commutator^{2,3,11} of the operators: $C(t) = \langle |[W(t), V]|^2 \rangle = 2(1 - \text{Re} F(t))$. If W and V are far apart local operators, then their squared commutator $C(t)$ should vanish initially (for $t = 0$). As time evolves, the operator $W(t)$ will grow in size and complexity, and eventually spread to the location of the operator V , at which point $C(t)$ develops a finite value. So the growth of the squared commutator $C(t)$, or the decay of the OTOC $F(t)$, characterizes the growth of local operators and the spreading of quantum information, which is a phenomenon known as scrambling¹⁸⁻²¹. Typically, the OTOC will remain large until the scrambling time²⁰ t_{scr} and decay rapidly once $t > t_{\text{scr}}$. The scrambling time t_{scr} generally depends on the distance d_{WV} between W and V operators. If we treat W as a perturbation to the system, then the OTOC also describes how a local perturbation W spreads to affect the measurement of V at a distance d_{WV} , which can be viewed as a quantum version of the butterfly effect.² The function $t_{\text{scr}}(d_{WV})$ describes the onset of the butterfly effect in space-time and traces out the boundary of the butterfly light-cone.

Although the OTOC was originally proposed to diagnose quantum chaos, recently there has been a growing interest to study the OTOC in non-chaotic quantum many-body systems as well, such as in rational conformal field theories^{13,22} and in many-body localized (MBL) systems²³⁻²⁸. In MBL systems,²⁹⁻³⁴ en-

ergy, charge, and other local conserved quantities can not diffuse due to the localization of excitations in the presence of strong disorder. Nevertheless, the quantum information can still propagate, as first demonstrated by the unbounded growth of entanglement³⁵⁻³⁹ after a global quench. The propagation of quantum information in MBL systems was also observed from OTOC measurements.^{23,24,27} Compared to quantum chaotic systems, where the scrambling time scales linearly with the spatial separation between the operators $t_{\text{scr}} \sim d_{WV}$, MBL systems were found to be a much slower scrambler with a scrambling time that scales exponentially with the operator separation $t_{\text{scr}} \sim \exp(d_{WV}/\xi)$. On the other hand, it was conjectured⁴⁰ that quantum critical fluctuations can enhance scrambling in chaotic systems. In this work, we found that criticality also enhances scrambling in non-chaotic MBL systems. We will demonstrate that the scrambling time follows a stretched exponential scaling $t_{\text{scr}} \sim \exp(\sqrt{d_{WV}/l_0})$ for marginal MBL systems⁴¹ (i.e. quantum critical MBL systems), which is different from both the quantum chaotic and the MBL behaviors mentioned above.

We used the spectrum bifurcation renormalization group (SBRG)^{42,43} approach to calculate the OTOC in MBL and marginal MBL systems. SBRG is an efficient numerical approach to construct the MBL effective Hamiltonian from a given disordered quantum many-body Hamiltonian. The idea of SBRG is similar to the real space renormalization group for excited states (RSRG-X)⁴⁴⁻⁴⁹. At each RG step, the leading energy scale term H_0 in the Hamiltonian is identified and the whole Hamiltonian is rotated to the (block) diagonal basis of H_0 ; then the terms in the off-diagonal blocks are reduced by the 2nd order perturbation. SBRG uses Clifford gates to boost the calculation efficiency for qubit models, such that the full spectrum is obtained in one run of RG (in contrast to RSRG-X which targets a single eigenstate at a time). With SBRG we can push the calculation of OTOC to much larger system size (e.g. 256 spins in this work) than exact diagonalization, hence verifying the scaling behaviors of the butterfly light-cones over a much larger scale.

We start by deriving the formula for the OTOC that

can be used in the SBRG calculations. The output of SBRG⁴² is the MBL effective Hamiltonian,^{38,45,50–54} which can be written in terms of the stabilizers (1-bits) τ_a^z ($a = 1, 2, \dots, L$ labels the stabilizers) as,

$$H_{\text{MBL}} = \sum_a \epsilon_a \tau_a^z + \sum_{a,b} \epsilon_{ab} \tau_a^z \tau_b^z + \sum_{a,b,c} \epsilon_{abc} \tau_a^z \tau_b^z \tau_c^z \dots, \quad (2)$$

which contains single-body terms $\epsilon_a \tau_a^z$, two-body terms $\epsilon_{ab} \tau_a^z \tau_b^z$ and higher-body terms. The key difference between Anderson and MBL insulators is that the two-body and higher-body terms are absent in the former while present in the later. H_{MBL} can also describe the marginal MBL system, where the major modification is that the stabilizers τ_a^z will be quasi-long-ranged (The chance of finding a stabilizer decays as a power-law with its length), instead of exponentially localized in the MBL system.

The stabilizers all commute with each other and also commute with the Hamiltonian, i.e. $[\tau_a^z, \tau_b^z] = [\tau_a^z, H_{\text{MBL}}] = 0$. To simplify the notation, we denote each product of stabilizers as $\tau_{abc\dots}^z = \tau_a^z \tau_b^z \tau_c^z \dots$. We may further bundle the subscript indices together and write

$$H_{\text{MBL}} = \sum_A \epsilon_A \tau_A^z, \quad (3)$$

where $A = abc\dots$ stands for a sequence of stabilizer indices and $\tau_A^z = \prod_{a \in A} \tau_a^z$. Since the Hamiltonian H_{MBL} is a sum of commuting terms $\epsilon_A \tau_A^z$, the time-evolution operator $U(t)$ can be factorized to the product of unitary operators generated by every τ_A^z operator independently,

$$U(t) = e^{-itH_{\text{MBL}}} = \prod_{\tau_A^z} e^{-it\epsilon_A \tau_A^z}. \quad (4)$$

The product runs over all τ_A^z operators in the Hamiltonian H_{MBL} . The time-dependent operator $W(t)$ is then given by $W(t) = U(t)^\dagger W U(t)$.

We begin by transforming the W and V operators to the τ^z basis, which involves a unitary transformation composed of Clifford rotations with perturbative Schrieffer-Wolff corrections⁴². In this basis, W and V are then linear combinations of products of Pauli operators. For simplicity, we will neglect the perturbative Schrieffer-Wolff corrections, which are small in the limit of large disorder. In Ref. 42 we tested this approximation by restoring the many-body wave function from the Clifford rotation only, and benchmarking the result with exact diagonalization. Good wave function fidelity is achieved as long as the disorder is strong. We will only consider W and V which are products of Pauli operators (called *Pauli strings*) in the physical basis, which implies that they will remain Pauli strings in the τ^z basis (since Clifford rotations map Pauli strings to Pauli strings). Therefore their algebraic relations with τ_A^z is rather simple: W and V can either commute or anticommute with τ_A^z ⁷¹. Let \mathcal{C}_W (or \mathcal{A}_W) be the set of τ_A^z that *commute* (or *anticommute*)

with W . Any τ_A^z in H_{MBL} either belongs to \mathcal{C}_W or \mathcal{A}_W for any given W . With this setup, we can calculate the time-evolution of W as follows

$$\begin{aligned} W(t) &= \prod_{\tau_A^z} e^{it\epsilon_A \tau_A^z} W \prod_{\tau_A^z} e^{-it\epsilon_A \tau_A^z} \\ &= W \prod_{\tau_A^z \in \mathcal{A}_W} e^{-2it\epsilon_A \tau_A^z}. \end{aligned} \quad (5)$$

The unitary operators generated by $\tau_A^z \in \mathcal{C}_W$ will annihilate each other by commuting through W , so only those generated by $\tau_A^z \in \mathcal{A}_W$ will survive. Suppose W is a local operator (e.g. an on-site Pauli operator); then Eq. 5 indicates that the support (or the size) of $W(t)$ will grow in time. $W(t)$ starts out with $W(0) = W$ initially, and as time evolves, W will expand via a product of non-local operators $e^{-2it\epsilon_A \tau_A^z}$. Each of them gradually evolves from 1 to $i\tau_A^z$ in the time scale $\sim \epsilon_A^{-1}$. τ_A^z terms that are more non-local typically have smaller energy scales ϵ_A in the local Hamiltonian H_{MBL} , and thus take longer time to contribute to $W(t)$. So the operator $W(t)$ will grow gradually. Accordingly, as $W(t)$ becomes non-local, the quantum information associated with W will be spread throughout the system and can not be retrieved by local measurements, which illustrates the idea of quantum chaos^{7,12,55,56} and scrambling^{18–20}.

The OTOC was proposed to quantify the growth of the operator and the scrambling effect. Here let us discuss the OTOC at “infinite temperature” where the density matrix of the system is simply identity, so that

$$F(t) = \text{Tr } W(t)V(0)W(t)V(0), \quad (6)$$

(the daggers are omitted as we assume both W and V are Hermitian Pauli operators). Following the similar calculation in Eq. 5, we find

$$F(t) = \text{Tr } W V W V \prod_{\tau_A^z \in \mathcal{A}_W \cap \mathcal{A}_V} e^{4it\epsilon_A \tau_A^z}, \quad (7)$$

where τ_A^z are the terms in H_{MBL} that anticommute with both W and V . As both W and V are Pauli strings, regardless of whether they commute or anticommute, this just amounts to an overall sign in $W V W V = \pm 1$, which is not important. So we might as well assume $[W, V] = 0$ (which is the case for far apart local operators), then the OTOC simply reads $F(t) = \text{Tr } \prod_{\tau_A^z \in \mathcal{A}_W \cap \mathcal{A}_V} e^{4it\epsilon_A \tau_A^z}$. The unitary operators can be expanded, i.e.

$$F(t) = \text{Tr} \prod_{\tau_A^z \in \mathcal{A}_W \cap \mathcal{A}_V} (\cos(4\epsilon_A t) + i\tau_A^z \sin(4\epsilon_A t)). \quad (8)$$

We take an approximation by dropping all the $\sin(4\epsilon_A t)$ terms in the expansion (to be justified shortly),^{24,26} and arrive at a simple formula for the OTOC of MBL and marginal MBL systems,

$$F(t) \simeq \prod_{\tau_A^z \in \mathcal{A}_W \cap \mathcal{A}_V} \cos(4\epsilon_A t). \quad (9)$$

In numerics, we first run the SBRG on a given quantum many-body Hamiltonian to generate the MBL effective Hamiltonian H_{MBL} . From H_{MBL} we filter out all terms $\epsilon_A \tau_A^z$ that anticommute with both W and V (recall that W and V are Pauli strings in the τ_A^z basis since we dropped the perturbative Schrieffer-Wolff corrections) and collect their energy coefficients ϵ_A . Then the OTOC can be evaluated very efficiently according to Eq. 9. We must bear in mind that Eq. 9 does not apply to the thermalized system, because our starting point, the MBL effective Hamiltonian H_{MBL} , breaks down in the thermalized phase.

The approximation we made in Eq. 9 is to drop all terms in the expansion that contain the product of $\sin(4\epsilon_A t)$. Such terms will only arise when several different τ_A^z operators product to identity so as to survive the trace. However note that all τ_A^z in Eq. 9 are taken from the set $\mathcal{A}_W \cap \mathcal{A}_V$, within which one must have at least four τ_A^z product together to reach the identity (as long as W and V commute). Thus the $\sin(4\epsilon_A t)$ factors appear as products of four or more, whose short-time behavior is suppressed by $\sim t^4$ (as $t \rightarrow 0$). In conclusion, such terms will never dominate the expansion until after t_{scr} .

To calculate the OTOC of more general operators W and V , or to include the perturbative Schrieffer-Wolff corrections, one can expand the operators as a sum of Pauli strings in the τ^z basis, and express the OTOC as a sum of these operators. In the following, we will only focus on the OTOC of Pauli strings without Schrieffer-Wolff corrections.

The OTOC starts out at 1 and decays to 0. The time for the onset of the decay is defined as the scrambling time t_{scr} .^{15,20} One can estimate the scrambling time based on Eq. 9. At short-time, $\cos(4\epsilon_A t)$ can be Taylor expanded to $1 - \frac{1}{2}(4\epsilon_A t)^2 + \dots$, so the OTOC behaves as

$$F(t) = 1 - \frac{1}{2}(4\|\epsilon_A\|_{W,V}t)^2 + \dots, \quad (10)$$

where the energy scale $\|\epsilon_A\|_{W,V}$ is defined via

$$\|\epsilon_A\|_{W,V}^2 = \sum_{\tau_A^z \in \mathcal{A}_W \cap \mathcal{A}_V} \epsilon_A^2. \quad (11)$$

So the scrambling time t_{scr} is set by this energy scale as $t_{\text{scr}} = \|\epsilon_A\|_{W,V}^{-1}$. The energy scale $\|\epsilon_A\|_{W,V}$ is not just a Frobenius norm of the energy coefficients in H_{MBL} , it also sensitively depends on the operators W and V . If W and V are local operators, then the scrambling time scales only with the distance d_{WV} between W and V . The scaling behavior can be used to distinguish Anderson localization, MBL, marginal MBL and ergodic⁵⁷⁻⁶⁰ systems, as concluded in Tab. I.

For Anderson insulators, if the spacial separation between W and V is much greater than the localization length, then $\mathcal{A}_W \cap \mathcal{A}_V$ is usually an empty set, i.e. there is almost no stabilizer that can anticommute with both W and V because all stabilizers are exponentially

TABLE I: Scaling of scrambling time t_{scr} with the operator distance d_{WV} as $d_{WV} \rightarrow \infty$ in different types of systems.

	Anderson	MBL	Marginal MBL	Ergodic
$\ln t_{\text{scr}}$	∞	$\sim d_{WV}$	$\sim d_{WV}^{1/2}$	$\ln d_{WV}$

localized within the localization length. (Recall that all terms in H_{MBL} (Eq. 2) are stabilizers for Anderson insulators, and that we're approximating the stabilizers as a product of Pauli operators by neglecting the perturbative corrections.) In this case $\|\epsilon_A\|_{W,V} \rightarrow 0$ and hence $t_{\text{scr}} \rightarrow \infty$. So the OTOC will remain finite and not decay in time for far apart W and V , meaning that there is no scrambling in Anderson insulators.

The situation is different if we add interactions. For MBL systems, far apart W and V operators can be connected by many-body interaction terms in H_{MBL} . A typical contribution comes from the two-body terms $\epsilon_{ab} \tau_a^z \tau_b^z$ with τ_a^z localized around W and τ_b^z localized around V . Then $\|\epsilon_A\|_{W,V} \simeq \|\epsilon_{ab}\| \sim e^{-x_{ab}/\xi}$, where x_{ab} is the distance between τ_a^z and τ_b^z , which is also roughly the distance d_{WV} between W and V . So the scrambling time t_{scr} follows $\ln t_{\text{scr}} \sim d_{WV}/\xi$, leading to a logarithmic butterfly light-cone in the MBL system.²³⁻²⁷

Another direction out of Anderson insulators is to consider quantum critical systems, i.e. marginal MBL systems. In these systems, each stabilizer τ_a^z itself becomes power-law quasi localized, and can connect spatially far separated W and V . Then the energy scale can be dominated by the single-body energy $\|\epsilon_A\|_{W,V} \simeq \|\epsilon_a\| \sim e^{-\sqrt{l/l_0}}$, which follows the ‘‘stretched exponential’’ scaling with respect to the length l of the stabilizer (where l_0 is a length scale depending on the initial disorder strength). This scaling is an exact result in the free limit by RSRG and has been shown to apply to interacting cases in Fig. 2 as well in Ref. 42. l is also roughly the distance d_{WV} between W and V . Therefore the scrambling time t_{scr} follows $\ln t_{\text{scr}} \sim \sqrt{d_{WV}}$, leading to a squared logarithmic butterfly light-cone in the marginal MBL system. Because the scrambling in the marginal MBL system is determined by the single-body energy scale, the butterfly light-cone is not much affected by the absence or presence of the interaction.

To verify the above theoretical proposals, we numerically measure the OTOC in MBL and marginal MBL systems by SBRG. The model we study is the XYZ spin chain with strong disorder on a periodic 1D lattice. The Hamiltonian is given by⁴³

$$H = \sum_{i=1}^L (J_{i,x} \sigma_i^x \sigma_{i+1}^x + J_{i,y} \sigma_i^y \sigma_{i+1}^y + J_{i,z} \sigma_i^z \sigma_{i+1}^z), \quad (12)$$

where σ_i^μ ($\mu = x, y, z$) are the spin operators on i th site of a 1D lattice of length $L = 256$. The random couplings $J_{i,\mu} \in [0, J_\mu]$ are independently drawn from the power-law distribution $\text{PDF}(J_{i,\mu}) = 1/(\Gamma J_{i,\mu})(J_{i,\mu}/J_\mu)^{1/\Gamma}$,

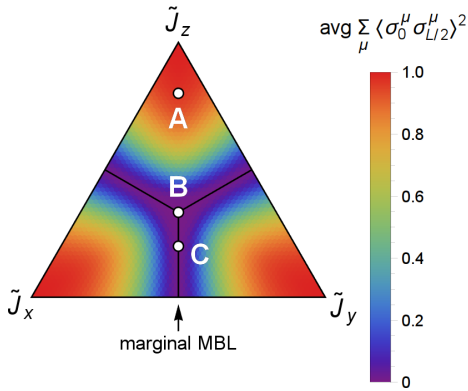


FIG. 1: A ternary plot (copied from⁴³) of the disorder and energy averaged Edwards-Anderson correlator vs coupling constants ($0 < \tilde{J}_{x,y,z} < 1$) for the XYZ spin chain of length $L = 256$. We use this plot to sketch the phase diagram. When $\tilde{J}_z > \max(\tilde{J}_x, \tilde{J}_y)$, the system is in an MBL \mathbb{Z}_2 spin glass state. When $\tilde{J}_z < \tilde{J}_x = \tilde{J}_y$, the system is in a marginal MBL phase. (The other phases are given by permutations of x, y, z .) The white dots correspond to the points in the phase diagram that are shown in Fig. 3.

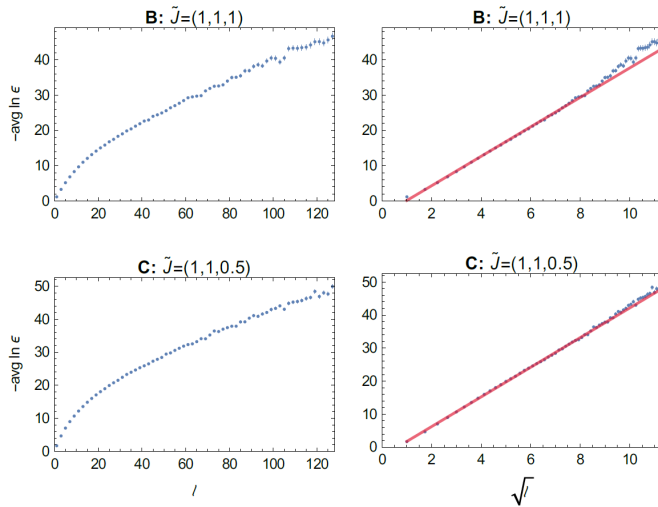


FIG. 2: Disorder average of the log of the stabilizer energy $\ln \epsilon$ vs stabilizer length ℓ on a periodic lattice of 256 spins in the marginal MBL phase of the XYZ spin chain. This figure verifies the scaling $-\ln \epsilon \sim \sqrt{\ell}$. The two rows (of plots) correspond to different points (B and C) in the phase diagram Fig. 1 while the two columns correspond to different horizontal axes: $|i-j|$ vs $\sqrt{|i-j|}$. (The fully MBL point (A) is not shown since it is deep in the MBL phase where nearly all stabilizers are of very short length.) The stabilizer length is calculated by writing a stabilizer τ_a^z in the physical basis and dropping all perturbative Schrieffer-Wolff corrections. The result is a product of Pauli operators at different sites. The stabilizer length is then the length of the shortest continuous sequence of sites (on the periodic lattice) that contains all of the Pauli operators. (Due to a slight even-odd effect, only odd stabilizer lengths are shown. 2^{16} disorder samples are used. Error bars denote one standard deviation statistical errors.)

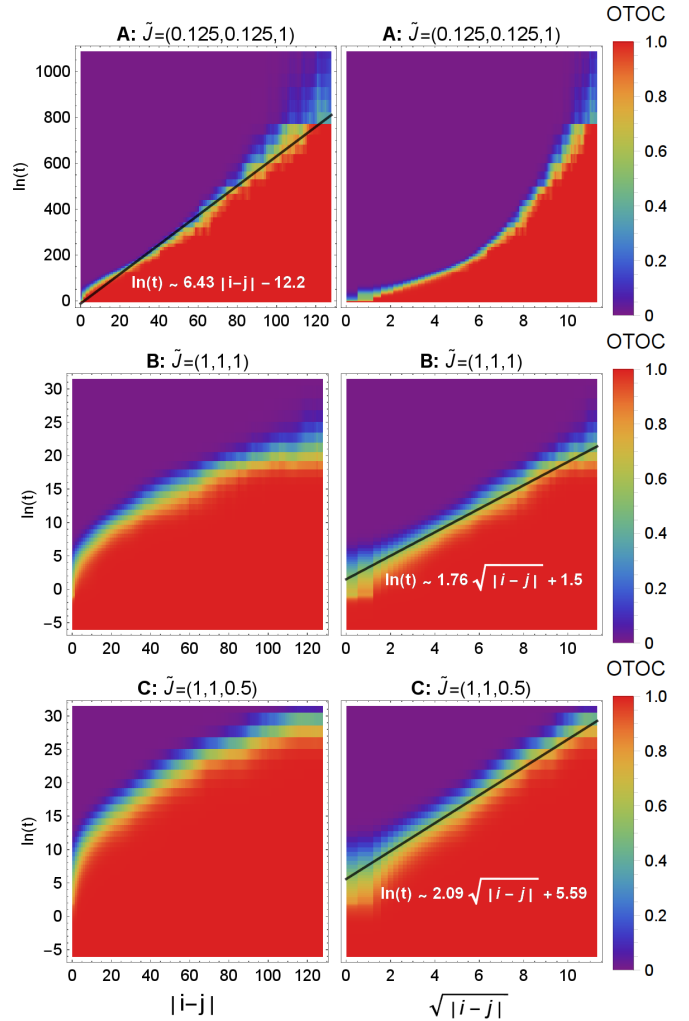


FIG. 3: Disorder average (using a geometric mean (Eq. 14)) of the out-of-time-order correlation (OTOC) (Eq. 6) $\exp \text{avg} \ln |F(t)|$ of $W = \sigma_i^x$ and $V = \sigma_j^y$ showing how the light cone of the (geometric mean) OTOC depends on the time t and distance $d_{WV} = |i-j|$ separation of W and V (on a lattice with 256 spins). Specifically, the light cone grows like $t_{\text{scr}} \sim \exp(\sqrt{d_{WV}/l_0})$. As in Fig. 2, the rows (of plots) correspond to different points in the phase diagram Fig. 1 while the two columns correspond to different horizontal axes: $|i-j|$ vs $\sqrt{|i-j|}$. Fits are shown for the cases when the scrambling time scaling agrees with the choice of horizontal axes. As can be seen from Fig. 4, the statistical errors and finite system size do not significantly affect the linear fit. (2^9 disorder samples are used.)

where $0 < \Gamma < \infty$ controls the disorder strength. We define

$$\tilde{J}_\mu \equiv J_\mu^{1/\Gamma}, \quad (13)$$

and take $\tilde{J} = (\tilde{J}_x, \tilde{J}_y, \tilde{J}_z)$ as the tuning parameters. In this work, a large disorder strength of $\Gamma = 4$ was used Ref. 43. The model has three spin glass MBL phases corresponding to the large \tilde{J}_x , \tilde{J}_y or \tilde{J}_z limits respectively, as shown in Fig. 1, where the spin flip $\mathbb{Z}_2 \times$

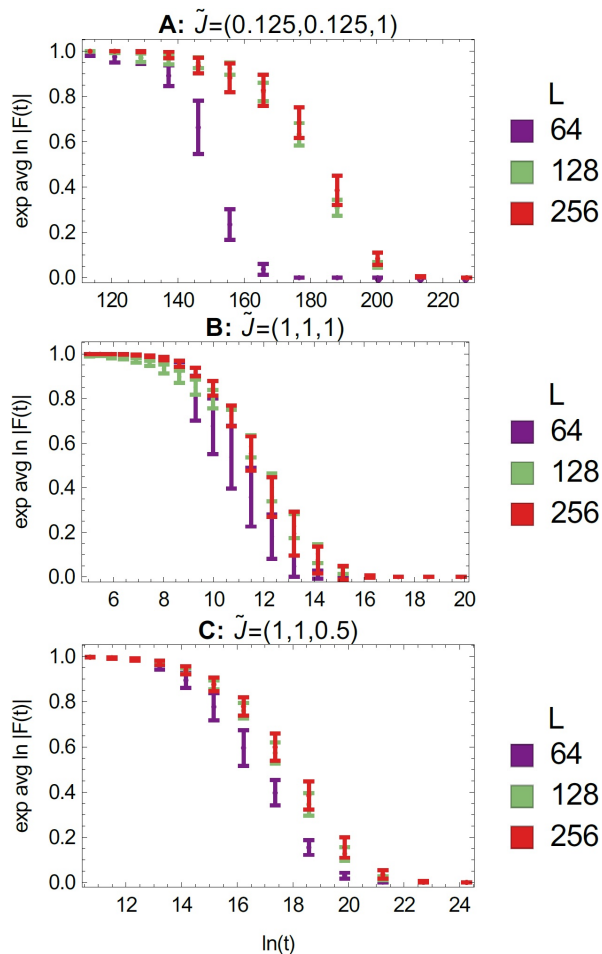


FIG. 4: A $d_{WV} = |i - j| = 32$ slice of Fig. 3 for different system sizes (and the same three points of the phase diagram Fig. 1). That is, we plot the disorder average (using a geometric mean (Eq. 14)) of the out-of-time-order correlation (OTOC) (Eq. 6) $\exp \text{avg} \ln |F(t)|$ of $W = \sigma_i^x$ and $V = \sigma_{i+32}^y$ for system sizes $L = 64, 128, 256$. We see that the OTOC for $|i - j| = 32$ converges very quickly with system size and has essentially completely converged by $L = 128$, which is only four times $|i - j|$. Thus, we expect Fig. 3 (for which $L = 256$) to have converged for all $|i - j| \leq 256/4 = 64$ (or $\sqrt{|i - j|} \leq 8$). Even when $L = 64$, which is only twice $|i - j|$, the OTOC has already mostly converged. Error bars are statistical errors which are calculated using the bootstrap method^{61,62} and are small enough to not have a significant effect on our light cone measurements.

\mathbb{Z}_2 symmetry is broken in every many-body eigenstate of the Hamiltonian. The spin glass phases are separated by three phase boundaries, where all the eigenstates become quantum critical, and the system is at the marginal MBL point.

We will focus along the line of $\tilde{J}_x = \tilde{J}_y$ and study the behavior of OTOC by SBRG. Details of the SBRG algorithm are given in Ref. 42,43. In short, SBRG can accurately simulate phases with spectrum bifurcation in the limit of large disorder where the Hamiltonian is

written as a sum of products of Pauli operators where each product of Pauli operators has an independently random coefficient. By large disorder, we mean that for every coefficient h_i , the standard deviation of $\log(h_i)$ is large. SBRG performs well in both the fully MBL and the marginal MBL phases. SBRG does not perform well in or near thermal phases. In this work we keep the largest 1024 additional terms during each RG step.⁷² Keeping more terms in Σ^2 was beneficial for this work because it allows SBRG to capture more of the small terms in H_{MBL} (Eq. 2), which allows us to more accurately calculate the OTOC at larger distances in Fig. 3.

In Fig. 3 we show the color plots of the OTOC $F(t) = \text{Tr} W(t)V(0)W(t)V(0)$ for local operators $W = \sigma_i^x$ and $V = \sigma_j^y$ at sites i and j respectively. The choice of the operators is quite generic. The primary consideration is to avoid the operators that commute with most of the local integral of motions (LIOMs) in the MBL system, else it is difficult to observe the decay of the OTOC within reasonable time scale.²³ As the LIOMs in the large- \tilde{J}_z spin glass phase are mainly $\sigma_i^z \sigma_{i+1}^z$, we will not choose W or V to be σ^z operators. Other than that, we have tried several different choices of W and V , and the resulting OTOC is similar to what is shown in Fig. 3.

In our calculation, the disorder averaging is done using a geometric mean (which measures the typical value of the OTOC). More specifically, we calculated

$$\exp \text{avg} \ln |F(t)| = \exp \left(\frac{1}{N_\delta} \sum_\delta \ln |F(t)| \right) \quad (14)$$

where \sum_δ denotes the summation over N_δ disorder samples. The typical correlation function in a marginal MBL phase, and its crucial difference from the arithmetic mean value (often dominated by rare events) was discussed in many previous studies⁶³⁻⁶⁶. In our case, the geometric mean was used because it was not possible to accurately calculate the ordinary mean at large time and distance separation using our SBRG methods. For a given disorder sample, sometimes SBRG does not manage to find enough terms in Eq. 9, which results in an $F(t)$ that is too large at large time t . This error can substantially affect the arithmetic mean of $|F(t)|$, but is negligible in the geometric mean. Therefore we use the typical OTOC (i.e. geometric mean) to reduce the rare-event effect.

We see in Fig. 3 that in general the OTOC starts out from 1 and decays to 0. The time-scale for the onset of the decay, i.e. the scrambling time t_{scr} , grows monotonically with the distance $d_{WV} = |i - j|$ between the operators W and V . The top row of Fig. 3 is deep in the MBL spin glass phase with $\tilde{J}_z/\tilde{J}_{x,y} = 8$, while the middle and bottom row are at the marginal MBL critical points with $\tilde{J}_x = \tilde{J}_y = \tilde{J}_z$ or $2\tilde{J}_z$ (see Fig. 1 for a phase diagram). The left column is plotted with $|i - j|$ as the horizontal axis, while the right column uses $\sqrt{|i - j|}$. The side-by-side comparison shows that in the MBL phase, the OTOC light cone is logarithmic

$\ln t_{\text{scr}} \sim d_{WV}$, while the marginal MBL light cone obeys $\ln t_{\text{scr}} \sim d_{WV}^{1/2}$, as expected. On the other hand, if we treat d_{WV} as a function of time:

$$d_{WV} \sim (\ln t)^2, \quad (15)$$

then d_{WV} can be viewed as the size of the operator $W(t)$. So Eq. 15 also describes the slow spreading of the quantum information of operator W in the system. Its transport universality class is known as the Sinai diffusion,⁶⁷ which governs the transport in critical Anderson localized system.⁶⁸ Our calculation demonstrates that the spreading of quantum information in marginal MBL systems also follows the Sinai diffusion rule. Interaction does not seem to affect the diffusion behavior, probably because the operator growth in the marginal MBL system is dominated by the single-body terms $\sum_a \epsilon_a \tau_a^z$ of the MBL Hamiltonian. The Sinai diffusion of quantum information is also seen in the entanglement growth $S(t) \sim (\ln t)^2$ for Ising-like marginal MBL systems, as studied in Ref. 44,48,69.

In summary, we demonstrated how the OTOC in MBL and marginal MBL systems can be efficiently calculated

using the SBRG approach. The system size can be pushed to several hundred sites, much larger than the previous exact diagonalization studies. We confirmed the logarithmic butterfly light cone $\ln t_{\text{scr}} \sim d_{WV}$ in the MBL system. We found the marginal MBL system is a faster scrambler due to quantum criticality. Its scrambling is dominated by single-body terms in the MBL effective Hamiltonian, which is different from the MBL cases. Therefore marginal MBL systems have a different butterfly light cone scaling $\ln t_{\text{scr}} \sim d_{WV}^{1/2}$. In this paper, we focused on the case where W and V are both local operators. Our calculation can be generalized to generic operators over regions of finite lengths.

Acknowledgement — We would like to thank Yingfei Gu, Xiao Chen, Xiao-Liang Qi, Yichen Huang, and Yu Chen for inspiring discussions. The authors are supported by the David and Lucile Packard Foundation and NSF Grant No. DMR-1151208. We acknowledge support from the Center for Scientific Computing from the CNSI, MRL: an NSF MRSEC (DMR-1121053) and NSF CNS-0960316.

-
- ¹ Y. N. Larkin, A.; Ovchinnikov, Sov. Phys. JETP **28**, 1200 (1969).
- ² S. H. Shenker and D. Stanford, Journal of High Energy Physics **3**, 67 (2014), 1306.0622.
- ³ A. Y. Kitaev (2014), talk at the Fundamental Physics Prize Symposium.
- ⁴ S. H. Shenker and D. Stanford, Journal of High Energy Physics **12**, 46 (2014), 1312.3296.
- ⁵ S. H. Shenker and D. Stanford, Journal of High Energy Physics **5**, 132 (2015), 1412.6087.
- ⁶ D. A. Roberts, D. Stanford, and L. Susskind, Journal of High Energy Physics **3**, 51 (2015), 1409.8180.
- ⁷ D. A. Roberts and D. Stanford, Physical Review Letters **115**, 131603 (2015), 1412.5123.
- ⁸ A. Kitaev (2015), talk at KITP Program: Entanglement in Strongly-Correlated Quantum Matter, URL <http://online.kitp.ucsb.edu/online/entangled15/kitaev/>.
- ⁹ J. Maldacena and D. Stanford, ArXiv e-prints (2016), 1604.07818.
- ¹⁰ J. Maldacena, D. Stanford, and Z. Yang, ArXiv e-prints (2016), 1606.01857.
- ¹¹ J. Maldacena, S. H. Shenker, and D. Stanford, Journal of High Energy Physics **8**, 106 (2016), 1503.01409.
- ¹² P. Hosur, X.-L. Qi, D. A. Roberts, and B. Yoshida, Journal of High Energy Physics **2**, 4 (2016), 1511.04021.
- ¹³ Y. Gu and X.-L. Qi, Journal of High Energy Physics **8**, 129 (2016), 1602.06543.
- ¹⁴ W. Fu and S. Sachdev, Phys. Rev. B **94**, 035135 (2016), 1603.05246.
- ¹⁵ B. Swingle, G. Bentsen, M. Schleier-Smith, and P. Hayden, ArXiv e-prints (2016), 1602.06271.
- ¹⁶ G. Zhu, M. Hafezi, and T. Grover, ArXiv e-prints (2016), 1607.00079.
- ¹⁷ N. Y. Yao, F. Grusdt, B. Swingle, M. D. Lukin, D. M. Stamper-Kurn, J. E. Moore, and E. A. Demler, ArXiv e-prints (2016), 1607.01801.
- ¹⁸ D. N. Page, Phys. Rev. Lett. **71**, 1291 (1993).
- ¹⁹ P. Hayden and J. Preskill, Journal of High Energy Physics **9**, 120 (2007), 0708.4025.
- ²⁰ Y. Sekino and L. Susskind, Journal of High Energy Physics **10**, 065 (2008), 0808.2096.
- ²¹ N. Lashkari, D. Stanford, M. Hastings, T. Osborne, and P. Hayden, Journal of High Energy Physics **4**, 22 (2013), 1111.6580.
- ²² P. Caputa, T. Numasawa, and A. Veliz-Osorio, ArXiv e-prints (2016), 1602.06542.
- ²³ Y. Huang, Y.-L. Zhang, and X. Chen, ArXiv e-prints (2016), 1608.01091.
- ²⁴ R. Fan, P. Zhang, H. Shen, and H. Zhai, ArXiv e-prints (2016), 1608.01914.
- ²⁵ B. Swingle and D. Chowdhury, ArXiv e-prints (2016), 1608.03280.
- ²⁶ Y. Chen, ArXiv e-prints (2016), 1608.02765.
- ²⁷ R.-Q. He and Z.-Y. Lu, ArXiv e-prints (2016), 1608.03586.
- ²⁸ X. Chen, T. Zhou, D. A. Huse, and E. Fradkin, ArXiv e-prints (2016), 1610.00220.
- ²⁹ R. Berkovits and Y. Avishai, Journal of Physics: Condensed Matter **8**, 389 (1996).
- ³⁰ R. Berkovits and Y. Avishai, arXiv preprint cond-mat/9707066 (1997).
- ³¹ I. V. Gornyi, A. D. Mirlin, and D. G. Polyakov, Physical Review Letters **95**, 206603 (2005), cond-mat/0506411.
- ³² D. M. Basko, I. L. Aleiner, and B. L. Altshuler, Annals of Physics **321**, 1126 (2006), cond-mat/0506617.
- ³³ J. Z. Imbrie, ArXiv e-prints (2014), 1403.7837.
- ³⁴ R. Nandkishore and D. A. Huse, Annual Review of Condensed Matter Physics **6**, 15 (2015), 1404.0686.
- ³⁵ J. H. Bardarson, F. Pollmann, and J. E. Moore, Physical

- Review Letters **109**, 017202 (2012), 1202.5532.
- ³⁶ G. DeChiara, S. Montangero, P. Calabrese, and R. Fazio, *Journal of Statistical Mechanics: Theory and Experiment* **3**, 03001 (2006), cond-mat/0512586.
- ³⁷ M. Žnidarič, T. Prosen, and P. Prelovšek, *Phys. Rev. B* **77**, 064426 (2008), 0706.2539.
- ³⁸ M. Serbyn, Z. Papić, and D. A. Abanin, *Physical Review Letters* **110**, 260601 (2013), 1304.4605.
- ³⁹ A. Nanduri, H. Kim, and D. A. Huse, *Phys. Rev. B* **90**, 064201 (2014), 1404.5216.
- ⁴⁰ H. Shen, P. Zhang, R. Fan, and H. Zhai, *ArXiv e-prints* (2016), 1608.02438.
- ⁴¹ R. Nandkishore and A. C. Potter, *Phys. Rev. B* **90**, 195115 (2014), 1406.0847.
- ⁴² Y.-Z. You, X.-L. Qi, and C. Xu, *ArXiv e-prints* (2015), 1508.03635.
- ⁴³ K. Slagle, Y.-Z. You, and C. Xu, *Phys. Rev. B* **94**, 014205 (2016), 1604.04283.
- ⁴⁴ R. Vosk and E. Altman, *Physical Review Letters* **110**, 067204 (2013), 1205.0026.
- ⁴⁵ B. Swingle, *ArXiv e-prints* (2013), 1307.0507.
- ⁴⁶ G. Refael and E. Altman, *Comptes Rendus Physique* **14**, 725 (2013), 1402.6008.
- ⁴⁷ D. Pekker, G. Refael, E. Altman, E. Demler, and V. Oganesyan, *Physical Review X* **4**, 011052 (2014), 1307.3253.
- ⁴⁸ R. Vasseur, A. C. Potter, and S. A. Parameswaran, *Physical Review Letters* **114**, 217201 (2015), 1410.6165.
- ⁴⁹ R. Vasseur, A. J. Friedman, S. A. Parameswaran, and A. C. Potter, *ArXiv e-prints* (2015), 1510.04282.
- ⁵⁰ M. Serbyn, Z. Papić, and D. A. Abanin, *Physical Review Letters* **111**, 127201 (2013), 1305.5554.
- ⁵¹ D. A. Huse, R. Nandkishore, and V. Oganesyan, *Phys. Rev. B* **90**, 174202 (2014), 1305.4915.
- ⁵² I. H. Kim, A. Chandran, and D. A. Abanin, *ArXiv e-prints* (2014), 1412.3073.
- ⁵³ A. Chandran, I. H. Kim, G. Vidal, and D. A. Abanin, *Phys. Rev. B* **91**, 085425 (2015), 1407.8480.
- ⁵⁴ L. Rademaker, *ArXiv e-prints* (2015), 1507.07276.
- ⁵⁵ M. Srednicki, *Phys. Rev. E* **50**, 888 (1994).
- ⁵⁶ L. F. Santos and M. Rigol, *Phys. Rev. E* **81**, 036206 (2010).
- ⁵⁷ S. A. Hartnoll, *Nature Physics* **11**, 54 (2015), 1405.3651.
- ⁵⁸ M. Blake, *ArXiv e-prints* (2016), 1603.08510.
- ⁵⁹ M. Blake, *ArXiv e-prints* (2016), 1604.01754.
- ⁶⁰ Y. Gu, X.-L. Qi, and D. Stanford, *ArXiv e-prints* (2016), 1609.07832.
- ⁶¹ S. X. Chen, W. Hrdle, and M. Li, *Journal of the Royal Statistical Society: Series B (Statistical Methodology)* **65**, 663 (2003), ISSN 1467-9868, URL <http://dx.doi.org/10.1111/1467-9868.00408>.
- ⁶² B. Efron, *Ann. Statist.* **7**, 1 (1979), URL <http://dx.doi.org/10.1214/aos/1176344552>.
- ⁶³ D. S. Fisher, *Phys. Rev. Lett.* **69**, 534 (1992).
- ⁶⁴ D. S. Fisher, *Phys. Rev. B* **50**, 3799 (1994).
- ⁶⁵ D. S. Fisher, *Phys. Rev. B* **51**, 6411 (1995).
- ⁶⁶ O. Motrunich, K. Damle, and D. A. Huse, *Phys. Rev. B* **63**, 134424 (2001), cond-mat/0005543.
- ⁶⁷ Y. G. Sinai, *Theory Probab. Appl.* **27** (1982).
- ⁶⁸ D. Bagrets, A. Altland, and A. Kamenev, *ArXiv e-prints* (2016), 1605.01657.
- ⁶⁹ R. Vosk and E. Altman, *Physical Review Letters* **112**, 217204 (2014), 1307.3256.
- ⁷⁰ S. Gopalakrishnan, M. Mueller, V. Khemani, M. Knap, E. Demler, and D. A. Huse, *ArXiv e-prints* (2015), 1502.07712.
- ⁷¹ In MBL phase or marginal MBL phase, W and V should be an infinite sum of Pauli strings in the τ basis, with coefficients decaying exponentially with both the disorder and the range^{51,70}, see for instance Fig.3 of Ref. 43. Neglecting the Schrieffer-Wolff correction keeps the leading Pauli string in this expansion.
- ⁷² That is, in this work we keep 1024 (instead of only 256 as in Ref.43) additional terms to Σ^2 ; see Appendix B in Ref.43.